omy of the Hand (Lippincott, Philadelphia, ed. 3, 1984), p. 159.
18. The terms power and precision grip have been redefined over the years [see C. Long, in *The Hand*, R. Tubiana, Ed. (Saunders, Philadelphia, 1981), pp. 427–440; M. Marzke and M. S. Shackley, *J. Hum. Evol.* **15**, 439 (1986)]. Long noted that "dextrous manipulation of objects by the thumb and fingers, or precision handling, has relatively few variations" (above, p. 436). These variations involve the thumb and different combinations of the four fingers in two, three, four, or five jawed grips. All precision handling, however, involves the thumb. Marzke and Shackley expanded on the definitions of Napier and Long and described a further subset of precision handling that in some cases involves the thumb as a buttress rather than as a fully opposing structure. The precision grasping adaptations described here and that are correlated with early bone and stone tool use reflect the enhanced role of the thumb and its musculature as part of a multi-jawed chuck. The more primitive precision handling that does not depend on a well-developed thumb, and where the base of the thumb serves as a buttress, is often observed in chimpanzee tool behavior such as the hammering of hard nuts in the Tai Forest of Ivory Coast. Thus, the more general concept of precision grasping of Napier (*13*) or precision handling (Long, above) would seem adequate to explain behavioral correlates of thumb morphology in apes and humans, and in fossil hominids.
19. Pygmy chimpanzees are from the Tervuren Museum and Department of Anatomical Sciences, State University of New York at Stony Brook. Common chimpanzees are from the American Museum of Natural History (AMNH), the Smithsonian Institution, and the Cleveland Museum of Natural History (CMNH). Gorillas are from AMNH and CMNH. Modern humans are drawn from the Todd Collection at CMNH. Fossil hominids include the following: AL 333w-39 (*A. afarensis* from Hadar), SKX 5020 (*P. robustus* from Swartkrans), SK 84 (*H. erectus* from Swartkrans), and Shanidar 4 (*H. s. neanderthalensis* from Shanidar Cave, Iraq). All fossil hominid measurements, except Shanidar 4, were taken from original specimens by the author. Measurements of Shanidar 4 were reported by E. Trinkaus, *The Shanidar Neandertals* (Academic Press, New York, 1983).
20. R. L. Susman, *Science* **240**, 781 (1988).
21. In apes there is a tendon from the common deep finger flexor mass [flexor digitorum profundus (FDP)] that mimics the tendon of the flexor pollicis longus in humans. This tendon does not represent a separate muscle to the thumb in apes. In lesser apes (gibbons and siamang) there is a muscle belly, but it is functionally coupled with the FDP. Our electromyography experiments on an adult female gibbon (*Hylobates lar*) did not elicit flexion of the thumb separate from flexion of the fingers, as is the case in humans. In a sample of 90 great apes (96% of orangutans, 72% of gorillas, 52% of chimpanzees), the flexor pollicis longus muscle was "rudimentary and functionless" [W. L. Straus, *Q. Rev. Biol.* **17**, 228 (1942)].
22. Ape hands reveal a contrasting morphology to those of humans. In apes, the fingers (digits II to V) rather than the thumb (digit I) have an enhanced musculature. Apes have a variable series of contrahentes muscles, often to digits IV and V and sometimes to digit II. Humans and apes all have a contrahentes to the thumb, called the adductor pollicis (see Fig. 3).
23. Stress (*S*) = Force (*F*)/Area (*A*). In the present case, stress is increased by an increase in the transarticular compressive forces (*F*) due to the addition of three muscles crossing the metacarpophalangeal joint. The effect of increasing force is mitigated by expanding the area (*A*) of the joint over which muscle forces are concentrated. Humans and other hominids that co-occur with stone and bone tools such as SKX 5020 (*P. robustus*), SK 84 (*H. erectus*), and Shanidar 4 (*H. s. neanderthalensis*) have an increased area, *A*, presumably because they have added one or all of the complement of human thumb muscles. AL 333w-39 (*A. afarensis*), which predates the appearance of stone tools, does not display metacarpophalangeal joint expansion and most likely lacked a "human" complement of thumb muscles.
24. The oldest stone tools associated with reliable radiometric dates are from East Africa, members E and F of the Shungura formation of the lower Omo Valley, and at Hadar, from the Kada Hadar member along the Gona River in Ethiopia. These sites are dated at around 2.5 Ma [H. Roche and J.-J. Tiercelin, *C. R. Acad. Sci. Paris* **284**, 1871 (1977); J. W. K. Harris, *Afr. Archeol. Rev.* **1**, 3 (1983); F. C. Howell, P. Haesaerts, J. de Heinzelin, *J. Hum. Evol.* **16**, 665 (1987)].
25. The question of whether refined precision grasping is indeed related to tool behavior and not simply small-object feeding is settled by the fact that *Theropithecus gelada*, the quintessential non–tool-using small object feeder [C. J. Jolly, *Man* **5**, 6 (1970)] lacks a hominid-like thumb.
26. J.-M. Le Minor, *Gegenbaurs Morphol. Jahrb.* **134**, 693 (1988).
27. I thank W. Jungers, D. Krause, S. Leigh, J. Stern, and K. Steudel for their comments and help; L. Betti-Nash for the illustrations; and C. K. Brain and B. Asfaw for permission to study early hominid fossils. Supported by NSF grants BNS 870687 and SBR 9209004.

2 May 1994; accepted 22 June 1994

Requirement of Transcription Factor PU.1 in the Development of Multiple Hematopoietic Lineages

Edward W. Scott, M. Celeste Simon, John Anastasi, Harinder Singh*

The transcription factor PU.1 is a hematopoietic-specific member of the *ets* family. Mice carrying a mutation in the *PU.1* locus were generated by gene targeting. Homozygous mutant embryos died at a late gestational stage. Mutant embryos produced normal numbers of megakaryocytes and erythroid progenitors, but some showed an impairment of erythroblast maturation. An invariant consequence of the mutation was a multilineage defect in the generation of progenitors for B and T lymphocytes, monocytes, and granulocytes. Thus, the developmental programs of lymphoid and myeloid lineages require a common genetic function likely acting at the level of a multipotential progenitor.

Hematopoiesis is a regulated developmental cascade that generates at least eight distinct lineages that differentiate into the mature cell types of the blood (*1*). The process is initiated by a self-renewing, pluripotential stem cell that generates a hierarchical array of developmental intermediates consisting of multipotent and monopotent progenitor cells. Most mature blood cell types have short life-spans and little or no proliferative capacity—therefore, they are continuously regenerated.

The transcription factor PU.1 is the product of the *PU.1-Spi1-Sfpi1* proto-oncogene (*2–4*). The *PU.1* gene is expressed specifically in hematopoietic tissues, particularly in the monocytic and B lymphoid lineages (*2*, *5*, *6*). Numerous presumptive PU.1 target genes have been identified in these lineages (*7–11*). Therefore, PU.1 has been suggested to control the differentiation of B lymphocytes and monocytes. Overexpression of PU.1 in erythroblasts is sufficient for their immortalization (*12*). Binding sites for PU.1 are present in intron 2 of the mouse β-major (β^M)–globin gene (*5*), in a region of altered chromatin structure in erythroid cells. Thus, PU.1 may also be required for the development of erythroid progenitors during hematopoiesis.

To genetically analyze the functions of PU.1, we engineered mice carrying a mutant allele using gene targeting in embryonic stem cells. The structure of the *PU.1* gene is depicted in Fig. 1A. Exon 5 encodes the DNA binding domain (*2*). The targeting vector (pES-PUT) was designed to delete this coding segment and to replace it with the positive selectable marker *PGK::neo* (Fig. 1A). To enrich for homologous recombination events, we used the negative selectable marker *PGK::TK* (*13*). The targeting construct was assembled with isogenic DNA segments (*14*). The *neo* gene was flanked by approximately 2 and 12 kb of *PU.1* homologous sequence on its 5′ and 3′ ends, respectively (Fig. 1A). Targeted CCE.1 embryonic stem (ES) cell clones were used to generate mice heterozygous for the *PU.1* mutation (*15*).

At 7 weeks of age, *PU.1* heterozygotes were mated to generate *PU.1* homozygous mutant progeny. Three-week-old pups were genotyped by Southern (DNA) blot analysis. Out of 31 progeny, 10 were wild type and 21 were heterozygotes. The absence of homozygous mutant progeny was highly significant ($P > 99.9\%$) and indicated that *PU.1* is an essential gene, disruption of which results in prenatal lethality. Embryos

E. W. Scott and H. Singh, Department of Molecular Genetics and Cell Biology and Howard Hughes Medical Institute, University of Chicago, Chicago, IL 60637, USA.
M. C. Simon, Department of Medicine and Howard Hughes Medical Institute, University of Chicago, Chicago, IL 60637, USA.
J. Anastasi, Department of Pathology, University of Chicago, Chicago, IL 60637, USA.
*To whom correspondence should be addressed.

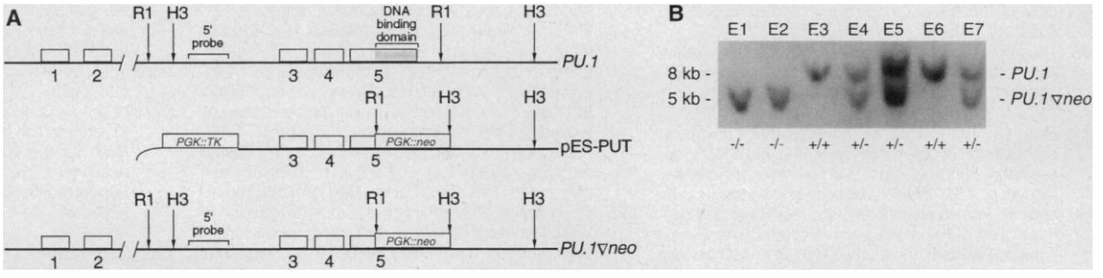

Fig. 1. *PU.1* targeting scheme and genotypic analysis. (**A**) The top, middle, and bottom line diagrams depict the structures of the *PU.1* gene, the pES-PUT targeting vector (*30*), and the *PU.1 neo* mutant allele generated by homologous recombination, respectively. Homologous recombination results in the replacement of the portion of exon 5 encoding the DNA binding domain of PU.1 (amino acids 200 to 272) by the *PGK::neo* selectable marker. Homologous recombination events can be screened because of the introduction of novel Eco RI (R1) and Hind III (H3) restriction sites in the *PU.1* locus. (**B**) Genotypic analysis of day 14.5 embryos (E1 through E7) from a mating of *PU.1* heterozygotes. Southern blot analysis was performed on Eco RI–digested DNA (*15*). Symbols are as follows: +/+, wild-type; +/−, heterozygote; and −/−, homozygous mutant.

representing various gestational ages were analyzed to determine when lethality occurred. Homozygous mutant embryos were present at the expected ratios until day 16.5 (see Fig. 1B for a sample litter). By day 17.5, mutant embryos were reduced in number, and no viable embryos were detected after day 18 of gestation.

PU.1 mutant embryos (days 14.5 to 17.5) exhibited an anemia of variable severity. The degree of anemia observed in the mutant embryos varied from being visually striking (hematocrit of 10%) to nondiscernible (hematocrit of 35%) (Fig. 2A). Hematocrit values for wild-type and heterozygous embryos were equivalent (40 ± 1.5%). In contrast, homozygous mutant embryos had a reduced hematocrit with significantly greater variability (25 ± 8.5%).

The anemia observed with *PU.1* mutant embryos suggested an impairment of fetal erythropoiesis. To examine the development of erythrocytes in the fetal liver, we fixed, sectioned, and stained (hematoxylin-eosin) the livers of wild-type and overtly anemic embryos (Fig. 2, C and D). In the wild-type fetal liver, proerythroblasts, erythroblasts, and pools of enucleated reticulocytes and erythrocytes were identified (Fig. 2C). In the fetal liver of an anemic mutant, proerythroblasts and erythroblasts were readily detectable; reticulocytes and erythrocytes were reduced in number and dispersed, rather than organized as pools of mature enucleated cells (Fig. 2D). Thus, maturation but not the generation of fetal erythroblasts was impaired by the *PU.1* mutation. The number of megakaryocytes in the fetal liver and platelets in the blood was unperturbed in mutant embryos (*16*).

PU.1 has been implicated in regulating the expression of the adult β^M-globin gene, which is initially activated in erythroblasts during fetal erythropoiesis. Ribonuclease protection analyses were done with a β^M riboprobe and RNA isolated from mutant (hematocrit of 15%), heterozygous, and wild-type embryos (Fig. 2B) (*17*). β^M-globin RNA was detected at equivalent amounts in each type of embryo. Therefore, *PU.1* is not required for the developmental activation of β-globin gene expression.

Murine B lymphocytes develop through a

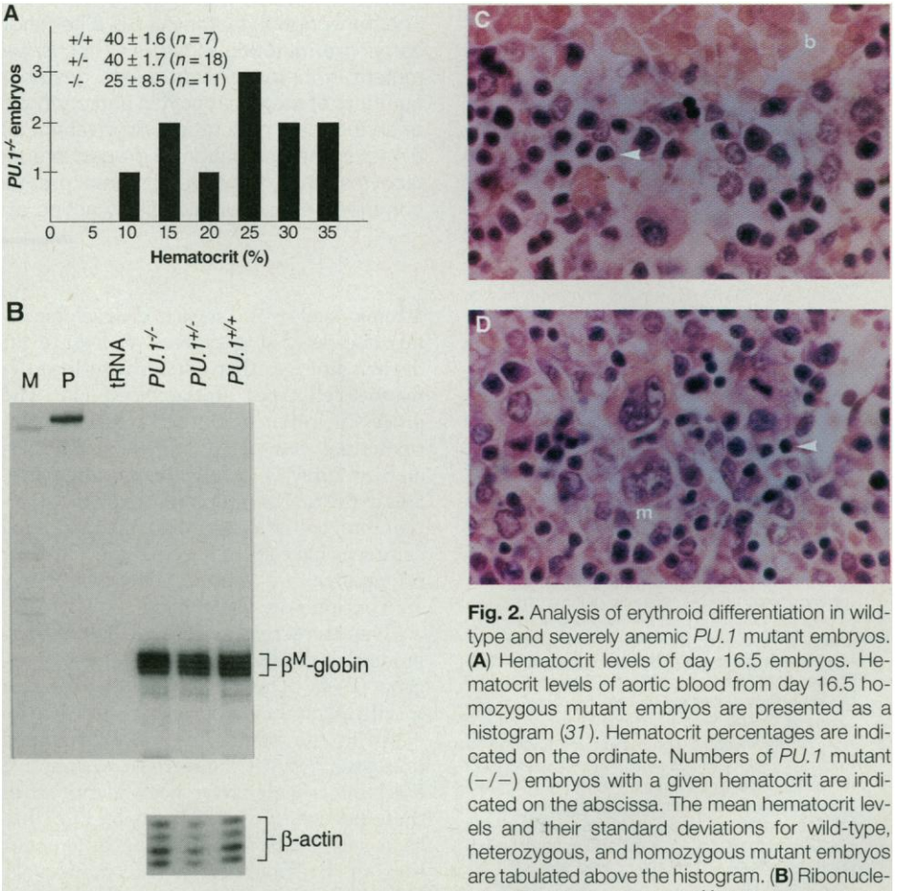

Fig. 2. Analysis of erythroid differentiation in wild-type and severely anemic *PU.1* mutant embryos. (**A**) Hematocrit levels of day 16.5 embryos. Hematocrit levels of aortic blood from day 16.5 homozygous mutant embryos are presented as a histogram (*31*). Hematocrit percentages are indicated on the ordinate. Numbers of *PU.1* mutant (−/−) embryos with a given hematocrit are indicated on the abscissa. The mean hematocrit levels and their standard deviations for wild-type, heterozygous, and homozygous mutant embryos are tabulated above the histogram. (**B**) Ribonuclease protection analysis of β^M-globin expression in wild-type, heterozygous, and *PU.1* mutant embryos. Total RNA was isolated from the fetal liver of wild-type (+/+), heterozygous (+/−), and *PU.1* mutant (−/−) littermates 16.5 days old (*17*). The wild-type and heterozygote embryos had a hematocrit level of 40%, whereas the *PU.1* mutant embryo exhibited a hematocrit level of 15%. RNA samples (10 μg) were hybridized to β^M-globin and actin antisense riboprobes (*17*). M, molecular weight markers; P, free probe; tRNA, control ribonuclease protection reaction using transfer RNA for hybridization. (**C** and **D**) Hematoxylin- and eosin-stained fetal liver sections from day 16.5 embryos (*23*). In (C), the wild-type fetal liver section demonstrates the presence of erythroid cells at various stages of maturation. Proerythroblasts and erythroblasts contain a prominent nucleus that stains dark purple (arrow). Reticulocytes and mature erythrocytes are reddish enucleated cells that are concentrated in pools (marked with b). In (D) is shown a *PU.1* mutant fetal liver section from a severely anemic littermate. Normal numbers of proerythroblasts and erythroblasts are present (arrow), but pools of reticulocytes and erythrocytes are absent. A megakaryocyte (m) is observable in the section of the *PU.1* mutant fetal liver.

series of well-defined intermediates. Progenitor B cells (pro-B), precursor B cells (pre-B), and mature B cells can be distinguished by the status of immunoglobulin (Ig) heavy and light chain gene rearrangements and expression of stage-specific cell surface markers (*18*). B cell development in the fetal liver is temporally ordered such that pro-B cells can be detected between days 12 and 13 of gestation, pre-B cells between days 14 to 16, and mature B cells between days 17 to 18 (*19*). Flow cytometry analysis (*20*) of B lineage cells in the fetal liver of embryos at day 16.5 showed that pro-B ($B220^+CD43^+$) and pre-B ($B220^+CD43^-$) cells were readily detected in both wild-type (Fig. 3A) and heterozygous embryos (*16*). However, these cells were not observed in the mutant embryos ($n = 14$) (Fig. 3A).

Immunoglobulin gene rearrangements and expression were analyzed by a reverse transcriptase–polymerase chain reaction assay (RT-PCR) (*17*). In the wild-type and heterozygous fetal livers (day 16.5), transcripts from Ig heavy chain alleles that had undergone D_μ-J_μ rearrangement were observed in large amounts (Fig. 3B). Though detectable, transcripts from Igκ alleles that had undergone V_κ-J_κ rearrangement were present in smaller amounts (Fig. 3B). No expression of D_μ-J_μ or V_κ-J_κ transcripts was detected in the fetal liver of *PU.1* mutant embryos. The difference in the V_κ-J_κ signals of the wild-type and heterozygous samples was not reproducible. Furthermore, no germline μ, *Rag1*, or *Rag2* transcripts were detected in *PU.1* mutant embryos (*16*). Thus, both transcription and rearrangement of Ig genes were blocked by the mutation. The *PU.1* mutation also resulted in the loss of expression of the B lineage–specific genes *mb-1*, *B29*, and *VpreB* (*16*). Therefore, on the basis of both the flow cytometry and RT-PCR analyses, disruption of the *PU.1* locus results in the elimination of B lineage progenitors.

The development of murine T lymphocytes, like that of B lymphocytes, involves both temporally ordered rearrangements of T cell receptor (TCR) gene segments and stage-specific expression of cell-surface markers (*21*). Flow cytometry was performed on fetal thymic cell suspensions (day 16.5) to determine the effect of the *PU.1* mutation on T lymphocyte development. In the wild-type thymus, differentiating thymocytes ($Thy\text{-}1^+CD2^-$ and $Thy\text{-}1^+CD2^+$) were detected in the expected numbers (Fig. 3A). In contrast, these cells were absent in the thymuses of mutant embryos. Additionally, whereas progenitors of the TCRαβ lineage ($CD4^+CD8^+$) constituted most of the thymocytes in the wild-type embryo, no such cells were present in the mutants (Fig. 3A). Consistent with the flow cytometry analysis, the thymuses of mutant embryos were hypocellular. These results are indicative of a requirement for *PU.1* at an early stage in T cell ontogeny.

Granulocytes (neutrophils) and monocytes-macrophages appear to arise from a common bipotential progenitor [granulocyte-macrophage colony-forming units (CFU-GM)] (*1*). The earliest morphologically identifiable precursors of each lineage are myeloblasts and monoblasts, respectively. Both precursors as well as mature cells of the granulocytic and monocytic lineages are observed in the fetal liver as early as day 13 of embryogenesis (*22*). The effect of the *PU.1* mutation on the development of granulocytes and monocytes was characterized by histological staining (*23*) and flow cytometry. In the wild-type fetal liver, developing granulocytic-monocytic cells were seen to express myeloperoxidase (blue granules, Fig. 4A) and lysozyme (red cytoplasm, Fig. 4C). These cells were completely absent in the fetal liver of mutant embryos (Fig. 4, B and D). Tissue macrophages, such as those found in the alveoli of lungs, were also eliminated by the *PU.1* mutation (*16*). Flow cytometry analysis of fetal liver suspensions (day 16.5 embryos) was done with antibodies to the β-integrin receptor (CD11b, CD18) and antibodies to Gr-1 (Fig. 4E). Wild-type fetal liver contained cells that expressed the β-integrin receptor, which is indicative of the granulocytic and monocytic lineages (Fig. 4E). No $CD11b^+CD18^+$ cells were detected in the *PU.1* mutant fetal liver ($n = 14$). This indicated a loss of both granulocytic and monocytic lineages. Consistent with this result, no mature granulocytes ($Gr\text{-}1^+$) were observed in the mutant embryos (Fig. 4E).

The effect of the *PU.1* mutation on hematopoietic progenitors was characterized with in vitro clonogenic assays (*24*). Wild-type and heterozygous fetal livers (day 14.5 to 15.5) yielded approximately 150 colonies per 10^6 cells representing CFU-GM (31%), CFU-GEMM (granulocyte-erythrocyte megakaryocyte-macrophage) (24%), CFU-G (granulocyte) (24%), CFU-M (macrophage) (17%), and CFU-

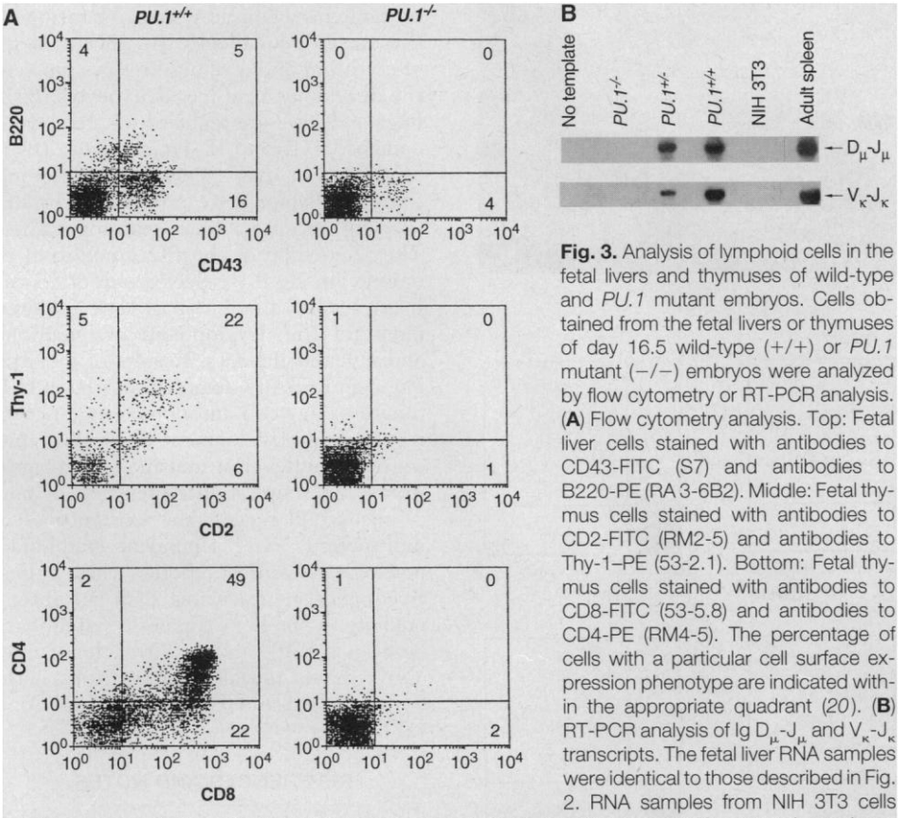

Fig. 3. Analysis of lymphoid cells in the fetal livers and thymuses of wild-type and *PU.1* mutant embryos. Cells obtained from the fetal livers or thymuses of day 16.5 wild-type (+/+) or *PU.1* mutant (−/−) embryos were analyzed by flow cytometry or RT-PCR analysis. (**A**) Flow cytometry analysis. Top: Fetal liver cells stained with antibodies to CD43-FITC (S7) and antibodies to B220-PE (RA 3-6B2). Middle: Fetal thymus cells stained with antibodies to CD2-FITC (RM2-5) and antibodies to Thy-1–PE (53-2.1). Bottom: Fetal thymus cells stained with antibodies to CD8-FITC (53-5.8) and antibodies to CD4-PE (RM4-5). The percentage of cells with a particular cell surface expression phenotype are indicated within the appropriate quadrant (*20*). (**B**) RT-PCR analysis of Ig D_μ-J_μ and V_κ-J_κ transcripts. The fetal liver RNA samples were identical to those described in Fig. 2. RNA samples from NIH 3T3 cells and the spleen of an adult wild-type mouse were used as negative and positive control templates, respectively. RT-PCR was performed on 5 μg of total RNA (*17*). Amplification products were analyzed by Southern blot hybridization with D_μ-J_μ or V_κ-J_κ probes. It should be noted that D_μ-J_μ transcripts were far more abundant than V_κ-J_κ transcripts in the fetal liver of wild-type and heterozygous embryos. The D_μ-J_μ blot was exposed to film for 5 min. The V_κ-J_κ blot, however, was exposed to film for 2 days, with the exception of the spleen sample, which was exposed for 5 min. Symbols are as follows: +/+, wild-type; +/−, heterozygote; and −/−, *PU.1* homozygous mutant.

Meg (megakaryocyte) (3%). The conditions used did not support the growth of CFU-E (erythrocyte) or of BFU-E (burst forming unit–erythrocyte). In contrast, the plating of fetal liver cells from *PU.1* homozygous mutant embryos yielded 5 to 10 colonies per 10^6 cells. These colonies were significantly smaller than those from wild-type cultures and primarily contained megakarocytes with some erythroid lineage cells. Mutation of *PU.1*, therefore, eliminates multipotential myeloid progenitors.

The expression of the *PU.1* gene appears restricted to cells of the hematopoietic system. Consistent with this pattern of expression, other aspects of embryogenesis, including the development of major organs (spleen, heart, kidney, lungs, and brain) and tissues (skin, muscle, and bone), appear to be unperturbed in the mutant embryos. The lymphoid-myeloid defects are specific to *PU.1* homozygous mutant embryos and are not observed in embryos heterozygous for the mutation. Thus, the engineered mutation represents a loss-of-function allele.

Mutation of the *PU.1* locus causes an invariant defect in the development of B and T lymphocytes, monocytes, and granulocytes. For each lineage, analysis with multiple stage-specific markers failed to reveal any differentiating intermediates. Because erythroid progenitors and megakaryocytes are generated in normal numbers in the *PU.1* mutant embryos, this multilineage defect is not simply a reflection of a *PU.1* requirement for the functioning of the hematopoietic stem cell. Although effects on B cell and monocyte development could be anticipated from previous work, the multilineage phenotype also shows a requirement for PU.1 for the generation of T lineage and granulocytic progenitors, and it reveals that in the B lineage PU.1 is not simply required for the activation of Ig heavy and κ light chain gene transcription. Instead, PU.1 is required for the development of B lineage progenitors that undergo Ig gene rearrangements and express the cell surface markers B220 and CD43 and the genes *mb-1*, *B29*, and *VpreB*. Thus, PU.1 is a pleiotropic regulator of B cell development acting at the earliest identifiable stage.

Only c-*myb*, *Rag1*, and *Rag2*, have been shown to be required for the development of multiple, but not all, lineages of the hematopoietic system. Mutation of the c-*myb* locus blocks the development of erythroid and myeloid lineages but not the development of megakaryocytes (*22*). *Rag1* and *Rag2* are required for the development of B and T lymphocytes (*25*). Mutations in these genes arrest differentiation of lymphocyte progenitors by inhibiting receptor gene rearrangements. The phenotype of the *PU.1* mutation is unique among this select group of genes. It establishes a common genetic requirement for the development of lymphoid and myeloid lineages. Results of in vitro clonogenic assays demonstrate that PU.1 functions in a cell-autonomous manner to regulate the development of myeloid lineages at the level of multipotent progenitors. The simplest interpretation of our results would suggest the existence of a multipotent, *PU.1*-dependent lymphoid-myeloid progenitor. Bone marrow–derived cells representing such an intermediate in the hematopoietic system can be cloned (*26*), and in vitro clonogenic assays have revealed progenitors with both myeloid and B lymphoid potential (*27*).

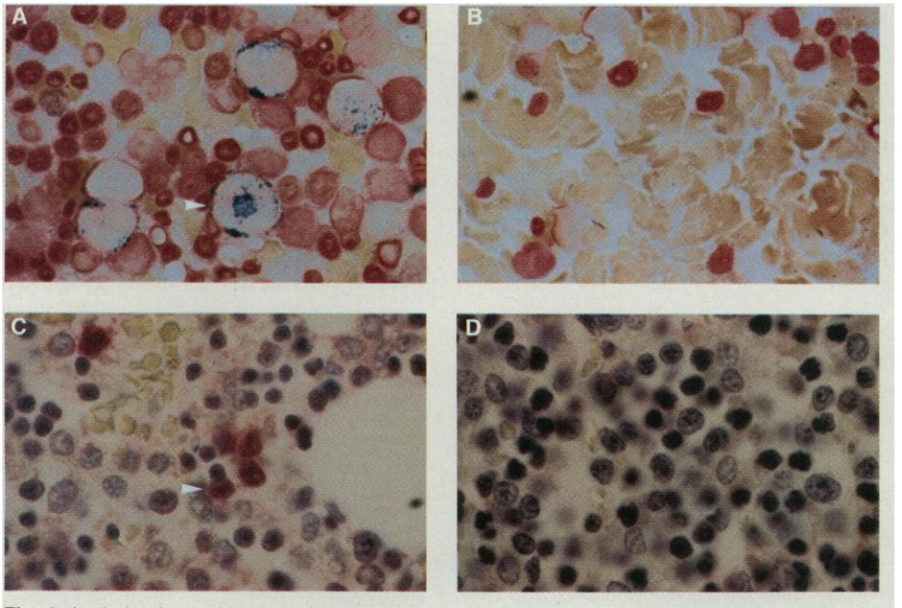

Fig. 4. Analysis of granulocytic and monocytic cells in the fetal liver of wild-type (+/+) and *PU.1* mutant (−/−) day 16.5 embryos. Shown in (A) through (D) is an analysis of myeloperoxidase- and lysozyme-expressing cells. Fetal liver touch preparations from wild-type (**A**) and homozygous mutant (**B**) littermates were stained for myeloperoxidase activity (*23*). Myeloperoxidase activity in wild-type fetal liver cells was visualized by the presence of blue cytoplasmic granules (arrow). Fetal liver sections from wild-type (**C**) and *PU.1* homozygous mutant (**D**) littermates were immunostained for lysozyme (*23*). Lysozyme-expressing cells in the wild-type fetal liver exhibit a dark red cytoplasm (arrow). (**E**) Flow cytometry analysis. Cells obtained from the fetal liver of wild-type (+/+) or *PU.1* mutant (−/−) embryos were analyzed by flow cytometry (*20*). Top: Fetal liver cells stained with antibodies to CD11b-FITC (M1/70) and antibodies to CD18-PE (C71/16). Bottom: Single-parameter fluorescence of fetal liver cells stained with antibody to Gr-1–FITC (RB6-8C5). The percentage of cells with a particular cell surface expression phenotype is indicated within the appropriate quadrant.

REFERENCES AND NOTES

1. G. Trinchieri, in *Neoplastic Hematopathology*, D. M. Knowles, Ed. (Williams & Wilkins, Baltimore, 1990).
2. M. J. Klemsz *et al.*, *Cell* **61**, 113 (1990); M. G. Goebl *et al.*, *ibid.*, p. 1165.
3. F. Moreau-Gachelin, A. Tavitian, P. Tambourin, *Nature* **331**, 277 (1988).
4. R. Paul *et al.*, *J. Virol.* **65**, 464 (1991).

5. D. L. Galson *et al.*, *Mol. Cell. Biol.* **13**, 2929 (1993).
6. R. Hromas *et al.*, *Blood* **82**, 2998 (1993).
7. B. Nelsen *et al.*, *Science* **261**, 82 (1993).
8. J. M. Pongubala *et al.*, *Mol. Cell. Biol.* **12**, 368 (1992); C. F. Eisenbeis, H. Singh, U. Storb, *ibid.* **13**, 6452 (1993).
9. J. Hagman and R. Grosschedl, *Proc. Natl. Acad. Sci. U.S.A.* **89**, 8889 (1992); A. L. Feldhaus *et al.*, *Mol. Cell. Biol.* **12**, 1126 (1992).
10. M. K. Shin and M. E. Koshland, *Genes Dev.* **7**, 2006 (1993).
11. D. E. Zhang, C. J. Hetherington, H. M. Chen, D. G. Tenen, *Mol. Cell. Biol.* **14**, 373 (1994); H. L. Pahl *et al.*, *J. Biol. Chem.* **268**, 5014 (1993).
12. S. Schuetze, P. E. Stenberg, D. Kabat, *Mol. Cell. Biol.* **13**, 5670 (1993).
13. S. L. Mansour, K. R. Thomas, M. R. Capecchi, *Nature* **336**, 348 (1988).
14. H. te Riele, E. R. Maandag, A. Berns, *Proc. Natl. Acad. Sci. U.S.A.* **89**, 5128 (1992).
15. CCE.1 ES cells were cultured under standard conditions [E. J. Robertson, *Teratocarcinomas and Embryonic Stem Cells: A Practical Approach* (IRL Press, Oxford, 1987)]. We electroporated ES cells (1×10^7) with Not I–linearized pES-PUT (30 μg) using a Bio-Rad Gene Pulsar apparatus (250 V, 500 μF) and placed them under selection [G418 (0.4 mg/ml; BRL) and gancyclovir (1 μM; Ross)] 24 hours after electroporation. Resistant colonies were picked and expanded in 24-well tissue culture plates. Genomic DNA was prepared and subjected to Southern blot analysis [F. M. Ausubel *et al.*, *Current Protocols in Molecular Biology* (Greene and Wiley-Interscience, New York, 1989)]. Hybridization and wash conditions were as described [E. W. Scott and H. V. Baker, *Mol. Cell. Biol.* **13**, 543 (1993)]. The *PU.1* probe used for hybridization corresponds to an 800-bp Kpn I fragment adjacent to the Kpn I fragment used in the targeting construct (Fig. 1A). Targeted clones representing a single integration event were injected into C57BL/6J blastocysts that were then implanted into CD-1 pseudopregnant female mice. Germline transmission of the ES cell genome was achieved with male chimeras derived from two independent clones. Analysis of tail DNA isolated from agouti progeny showed that 50% were heterozygous for the *PU.1* mutation. No apparent defects were manifest in the heterozygous animals when they were compared to wild-type littermates.
16. E. W. Scott and H. Singh, unpublished material.
17. RNA was isolated from fetal livers with RNAzol (Tel-Test, Friendswood, TX) according to the manufacturer's instructions. Ribonuclease protection assays were performed as described [C. L. Miller *et al.*, *Mol. Cell. Biol.* **11**, 4885 (1991)]. The β^M-globin riboprobe was as described [M. H. Baron and T. Maniatis, *Cell* **46**, 591 (1986)]. RT-PCR was performed as follows. First, we performed strand complementary DNA (cDNA) synthesis using 5 μg of RNA and random primers with a Pharmacia kit as per the manufacturer's instructions. PCR reactions for Ig gene transcripts were performed with either D_μ-J_μ primers (*28*) or V_κ-J_κ primers (*29*). PCR conditions were 30 cycles at 94°C for 30 s, 62°C for 30 s, and 72°C for 50 s. PCR products were resolved in 2% agarose gels and subjected to Southern blot analysis as described (*28*, *29*).
18. R. R. Hardy *et al.*, *J. Exp. Med.* **173**, 1213 (1991).
19. G. G. Lennon and R. P. Perry, *J. Immunol.* **144**, 1983 (1990); R. Palacios and J. Samaridis, *Mol. Cell. Biol.* **12**, 518 (1992).
20. Flow cytometry analysis was performed on single-cell suspensions of the fetal liver or thymus prepared by standard methodology [J. E. Coligan *et al.*, *Current Protocols in Immunology* (Greene and Wiley-Interscience, New York, 1993)]. Cells were stained with fluorescein isothiocyanate (FITC)– or phycoerythrin (PE)-conjugated antibodies and scanned on a FACScan (Becton Dickinson). Propidium iodide uptake and scatter-gating for size were used to exclude dead cells from analysis. Monoclonal antibodies [RA 3-6B2 (B220), S7 (CD43), 53-2.1 (Thy-1.2), RM2-5 (CD2), RM4-5 (CD4), 53-5.8 (CD8), RB6-8C5 (Gr-1), C71/16 (CD18), and M1/70 (CD11b)] were used according to the supplier's (PharMingen) instructions. Adult mouse spleen, bone marrow, and thymus suspensions were used as positive controls in setting staining gates.
21. E. V. Rothenberg, *Adv. Immunol.* **51**, 85 (1992).
22. M. L. Mucenski *et al.*, *Cell* **65**, 677 (1991).
23. Embryos were fixed in 4% paraformaldehyde and embedded in paraffin for sectioning. Hematoxylin and eosin staining was performed on embryo sections by standard methodology [W. J. Williams *et al.*, *Hematology* (McGraw-Hill, New York, 1990)]. Immunostaining for lysozyme was performed on fetal liver sections with a commercially available antibody as per the manufacturer's instructions (Dayco). Fetal liver touch preparations were stained for myeloperoxidase-positive cells by standard methodology.
24. Clonogenic assays were performed on single-cell suspensions of the fetal liver prepared as described for flow cytometry. Cells (2×10^5) were plated in 1.25 ml of complete MethoCult medium (Stemcell Tech., Vancouver, B.C., Canada) and incubated at 37°C in 5% CO_2. Colonies were counted and scored by morphology beginning on day 5 of culture. Colony identification was confirmed by histological staining of cytospin preparations.
25. P. Mombaerts *et al.*, *Cell* **68**, 869 (1992); Y. Shinkai *et al.*, *ibid.*, p. 855.
26. R. Palacios and J. Samaridis, *Blood* **81**, 1222 (1993).
27. A. Cumano, C. J. Paige, N. N. Iscove, G. Brady, *Nature* **356**, 612 (1992); F. Hirayama *et al.*, *Proc. Natl. Acad. Sci. U.S.A.* **89**, 5907 (1992).
28. M. S. Schlissel *et al.*, *J. Exp. Med.* **173**, 711 (1991).
29. M. S. Schlissel and D. Baltimore, *Cell* **58**, 1001 (1988).
30. A targeting vector cassette was created by cloning the *PGK::neo* gene from plasmid KJ-1 [M. W. McBurney *et al.*, *Nucleic Acids Res.* **20**, 5755 (1991)] into the Eco RI and Hind III sites of pTK-AB to generate pTK-neo. A *PU.1* cDNA (*2*) was used to isolate a 40-kb *PU.1* genomic DNA clone from a murine 129-SV cosmid library (Stratagene). A 1.7-kb Kpn I fragment containing exons 3 and 4 and a portion of exon 5 was inserted into pUC19. This *PU.1*–Kpn I fragment deletes 73 amino acids from the COOH-terminus of PU.1 (amino acids 200 to 272), which are required for DNA binding. The fragment was then inserted as an Xba I–Eco RI segment upstream of the *PGK::neo* gene of pTK-neo to generate pTK-5′-neo. A 14-kb Eco RI fragment, containing sequences immediately 3′ to exon 5 of *PU.1*, was subcloned into pBluescript SK (Stratagene). This *PU.1*–Eco RI fragment was then inserted as a Xho I–Not I segment into pTK-5′-neo to generate pES-PUT (Fig. 1A).
31. Peripheral blood was obtained from aortic bleeds. Hematocrit assays were performed essentially as described [M. D. Collins *et al.*, *Am. J. Physiol.* **257**, 542 (1989)].
32. We thank R. Maki for a *PU.1* cDNA clone; J. Bermingham, University of California, San Diego, for pTK-AB; F. Alt for low-passage CCE.1 cells; E. B. Crenshaw for experimental advice; P. Shah, J. Leiden, and C. Thompson for their critical review; and M. Min for histological preparations. Supported by the Howard Hughes Medical Institute (E.W.S. and H.S.). E.W.S. also acknowledges support from NIH grant F32 AI08933. M.C.S. was supported by an institutional American Cancer Society grant and the Cancer Foundation of Chicago. J.A. is a special fellow of the Leukemia Society of America.

10 May 1994; accepted 19 July 1994

Direct Observation of Enzyme Activity with the Atomic Force Microscope

Manfred Radmacher,* Monika Fritz,* Helen G. Hansma, Paul K. Hansma

The height fluctuations on top of the protein lysozyme adsorbed on mica were measured locally with an atomic force microscope operated in tapping mode in liquid. Height fluctuations of an apparent size of 1 nanometer that lasted for about 50 milliseconds were observed over lysozyme molecules when a substrate (oligoglycoside) was present. In the presence of the inhibitor chitobiose, these height fluctuations decreased to the level without the oligoglycoside. The most straightforward interpretation of these results is that the height fluctuations correspond to the conformational changes of lysozyme during hydrolysis. It is also possible, however, that the height fluctuations are, at least in part, the result of a different height or elasticity of the transient complex of lysozyme plus the substrate.

Since its invention, the atomic force microscope (AFM) (*1*) has been a promising tool for biological applications. In the last few years, proteins under physiological conditions (*2*) and live cells (*3*) have been imaged. In some instances, the AFM demonstrates true atomic resolution (*4*) and can detect the small forces of specific binding between individual molecules (*5*, *6*).

Recent progress in measuring and imaging the forces between proteins has been achieved with several techniques and systems (*6*, *7*). These measurements suggested that the state of the art of detecting small movements at very low forces would be sufficient for observing the motion of proteins at the molecular level. The advantage of the AFM is its combination of sensing small forces and its ability to position with nanometer accuracy and to detect objects at a molecular resolution. Enzymes are a very promising system for watching protein mo-

M. Radmacher, H. G. Hansma, P. K. Hansma, Department of Physics, University of California, Santa Barbara, CA 93106, USA.
M. Fritz, Department of Physics and Marine Science Institute, University of California, Santa Barbara, CA 93106, USA.
*To whom correspondence should be addressed.